

Proof Attempt of the Riemann Hypothesis via Zeropole Balance

Attila Csordas

Author Information

Name: Attila Csordas

Affiliation: AgeCurve Limited, Cambridge, UK

Email: attila@agecurve.xyz

ORCID: 0000-0003-3576-1793

Contents

1	Preamble	4
2	Mathematical Introduction	4
3	Preliminaries	6
3.1	Functional Equation of $\zeta(s)$	6
3.2	Hadamard Product Formula	7
3.2.1	Convergence of the Hadamard Product	7
3.3	Hardy's Theorem	9
3.4	Zeropole Mapping and Orthogonal Balance of $\zeta(s)$	9
4	Shadow Function Construction	10
4.1	Motivation	10

20	4.2	Definition of the Shadow Function	11
21	4.3	Exponential Stabilizer Properties	11
22	4.4	Numerical Validation	12
23	4.4.1	Zero Mean Condition for $\log \zeta^*(s)$ on the Critical Line	13
24	4.4.2	Growth Matching of $\log \zeta^*(s)$ with $\log \zeta(s)$ at Infinity	13
25	4.4.3	Key Differences Between the Two Validations	15
26	4.5	Proof of Convergence of the Shadow Function	16
27	4.6	Zeropole Mapping and Orthogonal Balance of $\zeta^*(s)$	17
28	5	Compactness of the Torus	18
29	5.1	Topological Preliminaries	18
30	5.2	Compactness via Open Cover Definition	18
31	5.3	Alternative Representation: Quotient of \mathbb{R}^2	19
32	6	Finite Periodic Divisor and Toroidal Embedding of $\zeta^*(s)$	19
33	6.1	Toroidal Embedding of $\zeta^*(s)$	20
34	6.2	Standard Divisor concept	20
35	6.3	Fundamental Domain Divisor Structure	21
36	6.3.1	Existence of Well-Defined Fundamental Domain Size	21
37	6.3.2	Generalized Divisor Valuation	22
38	6.3.3	Multi-Pole to Single-Zero Mapping Within Fundamental Domain	23
39	6.4	Bounded Fractional Contribution and Toroidal Periodicity	23
40	6.5	Application of Riemann-Roch with Periodic Divisors	24
41	6.6	Theoretical Justification for Bounded Fractional Contributions	24
42	6.6.1	Probability of an Irrational Zero Landing on a Rational Boundary	24
43	6.7	Fractional Contributions as a Safeguard	25

44	6.8	Finite, well-defined fundamental domain leads to global zeropole cancellation	25
45	7	Proof of Minimality, Exclusion of Off-Critical Zeros, and Uniqueness Lemma	26
46	7.1	Proof of Minimality	26
47	7.2	Exclusion of Off-Critical Zeros	26
48	7.3	Uniqueness of $\zeta^*(s)$ on the Torus	26
49	8	Conclusion: Proof of the Riemann Hypothesis	27
50	9	Geometric Riemann-Roch Interpretation for Shadow Function Global Unique-	
51		ness	27
52	9.1	Divisor Structure and Hyperplane Intersections on the Torus	28
53	9.2	Linear Independence and Orthogonality	28
54	9.3	Implications for Uniqueness and Minimality	28
55	10	Practical Dynamic Zero-Pole Pairing Algorithm for Local Regions	29
56	11	Numerical Validation of Dynamic Zero-Pole Pairing	32
57	11.1	Experimental Setup	32
58	11.2	Results and Interpretation	32
59	11.3	Reproducibility and Further Validation	33
60	12	Zeropole Balance as the Unifying Principle of the Proof	34
61	13	Balanced Zeropole Collapse via Sphere Eversion	37
62	14	Historical Remark	39
63	15	Acknowledgements	39
64	16	Supplementary Material	40

Abstract

This work presents a proof attempt for the Riemann Hypothesis (RH) via a toroidal compactification framework. By embedding the Riemann zeta's functions complete zero-pole structure into a genus-1 topology, we establish a finite fundamental domain divisor structure that ensures local zero-pole balance. This finite and periodic structure leads to global cancellation, providing a cohesive understanding of the distribution of non-trivial zeros and trivial poles. Our approach naturally encodes the functional equation and analytic continuation of $\zeta(s)$, leading to a minimality condition that excludes off-critical zeros. This method integrates geometrical, algebraic, analytical, and topological perspectives, unifying disparate aspects of zeta function theory into a cohesive framework. The toroidal compactification offers a novel structural perspective on RH, reinforcing zero-pole cancellation in a periodic setting.

1 Preamble

The Riemann Hypothesis (RH) is considered the most significant open problem in mathematics and the only major conjecture from the 19th century that remains unsolved. The default assumption among mathematicians is that every new proof attempt is likely false. Thus, the following proof will undergo immense scrutiny, which is both expected and necessary. Historically, the chances of a new proof being correct are incredibly low. Hence focusing on finding the possible technical issues with the following proof suggestion is very welcome. The majority opinion in the mathematical community is that the RH is very likely true and there's overwhelming evidence supporting it [Gow23]. It is only that the decisive, irreversible mathematical proof that is missing still.

2 Mathematical Introduction

The Riemann Hypothesis [Rie59], concerning the zeros of the analytically continued Riemann zeta function $\zeta(s)$, is a cornerstone of modern mathematics. Our proof attempt builds on classical results—including the Hadamard product formula and Hardy's theorem on zeros on the critical line—and leverages the concept of zero-pole mapping and orthogonal balance. This framework establishes a bijection and algebraic independence between trivial poles and non-trivial zeros of $\zeta(s)$, encoding their orthogonality in the complex plane. These properties provide a foundational structure for the proof and ensure a cohesive integration of geometrical, algebraic, and analytical perspectives. The Riemann zeta function $\zeta(s)$ is a complex function defined for complex numbers $s = \sigma + it$

98 with $\sigma > 1$ by the *Dirichlet series* representation:

$$\zeta(s) = \sum_{n=1}^{\infty} \frac{1}{n^s}.$$

99 This series collapses into the harmonic series and diverges at $s = 1$, see Euler's 1737
100 proof [Eul37], leading to a simple pole at this point, which is referred to as the *Dirich-*
101 *let pole*.

102 The non-trivial zeros of the Riemann zeta function are complex numbers with real parts
103 constrained in the critical strip $0 < \sigma < 1$:

104 The Riemann Hypothesis states that all non-trivial zeros of the Riemann zeta function lie
105 on the critical line:

$$\Re(s) = \sigma = \frac{1}{2}$$

106 In other words, the non-trivial zeros have the form:

$$s = \frac{1}{2} + it$$

107

108 The Riemann zeta function has a deep connection to prime numbers through the Euler
109 Product Formula (also known as the Golden Key), which is valid for $\Re(s) > 1$:

$$\zeta(s) = \prod_{p \text{ prime}} \frac{1}{1 - p^{-s}}$$

110 This formula expresses the zeta function as an infinite product over all prime numbers
111 p . It reflects the fundamental theorem of arithmetic, which states that every integer can
112 be factored uniquely into prime numbers. It shows that the behavior of $\zeta(s)$ is intimately
113 connected to the distribution of primes. Each term in the infinite prime product corresponds
114 to a geometric series for each prime p that captures the contribution of all powers of a single
115 prime p to the overall value of $\zeta(s)$. This representation of $\zeta(s)$ has made it a foundational
116 element of modern mathematics, particularly for its role in analytic number theory and the
117 study of prime numbers. However, our proof begins with the observation that the RH, as
118 originally formulated by Riemann, can be viewed purely as a complex analysis problem,
119 making it amenable to geometric, algebraic, and topological reformulations. The zeropole
120 framework focuses on the geometric and algebraic interplay between zeros and poles. Our
121 approach does not rely on the tools of analytical number theory, nor does it assume the
122 placement of non-trivial zeros along the critical line, thereby avoiding any potential circular
123 reasoning.

3 Preliminaries

3.1 Functional Equation of $\zeta(s)$

Theorem 1 (Functional Equation). *The Riemann zeta function satisfies the functional equation:*

$$\zeta(s) = 2^s \pi^{s-1} \sin\left(\frac{\pi s}{2}\right) \Gamma(1-s) \zeta(1-s).$$

Remark 1. *The trivial zeros of $\zeta(s)$ are located at $s = -2k$ for $k \in \mathbb{N}^+$. These zeros arise directly from the sine term in the functional equation:*

$$\sin\left(\frac{\pi s}{2}\right).$$

The sine function, $\sin(x)$, satisfies the periodicity property:

$$\sin(x + 2\pi) = \sin(x) \quad \text{for all } x \in \mathbb{R}.$$

Additionally, $\sin(x) = 0$ whenever $x = n\pi$ for $n \in \mathbb{Z}$.

Substituting $s = -2k$ into the argument of the sine function, we have:

$$\frac{\pi s}{2} = \frac{\pi(-2k)}{2} = -k\pi,$$

which is an integer multiple of π . Thus:

$$\sin\left(\frac{\pi s}{2}\right) = \sin(-k\pi) = 0.$$

This periodic vanishing of the sine function at $s = -2k$ dominates all other terms in the functional equation, such as $\Gamma(1-s)$ and $\zeta(1-s)$, ensuring that the zeta function itself vanishes at these points.

Therefore, the points $s = -2k$ ($k \in \mathbb{N}^+$) are classified as the trivial zeros of $\zeta(s)$, arising solely from the sine term's periodicity and its interplay within the functional equation.

Remark 2. *Introducing the **Zeropole Duality and Neutrality** principle as part of our conceptual zeropole framework: The Dirichlet pole of $\zeta(s)$ at $s = 1$ plays a dual role. In Theorem 1 establishing critical line symmetry, the term $\sin\left(\frac{\pi s}{2}\right)$ gives 0 at $s = 0$, while $\zeta(1-s)$ term retains the Dirichlet pole from $\zeta(1)$. This dual role exemplifies zeropole neutrality, where the pre-analytic continuation Dirichlet pole morphs into a balance of "zero-like" and "pole-like" contributions.*

These remarks establish the trivial zeros of $\zeta(s)$ and highlight the symmetry encoded in the functional equation as foundational elements for the zeropole framework.

3.2 Hadamard Product Formula

Theorem 2 (Hadamard Product Formula [Had93]). *The Riemann zeta function $\zeta(s)$ is expressed through the Hadamard product, which decomposes its zeropole structure as:*

$$\zeta(s) = \prod_{\rho} \left(1 - \frac{s}{\rho}\right) e^{s/\rho} \prod_{k=1}^{\infty} \left(1 - \frac{s}{-2k}\right)^{-1} \frac{s(1-s)}{\pi},$$

where:

- ρ ranges over all non-trivial zeros of $\zeta(s)$,
- The second infinite product explicitly accounts for trivial poles at $s = -2k$, arising from the modified interpretation of the Hadamard product,
- The $\frac{s(1-s)}{\pi}$ term encodes the Dirichlet pole's contribution as two "zero-like" terms at $s = 0$ and $s = 1$.

This decomposition encapsulates the complete zeropole structure of $\zeta(s)$.

Remark 3. *The Hadamard product formula explicitly encodes the orthogonal independence of trivial poles and non-trivial zeros of $\zeta(s)$. These two zeropole sets contribute as distinct infinite product terms, reflecting their algebraic and geometric independence. This orthogonality underpins the structural separation of these sets within the analytic continuation of $\zeta(s)$.*

Remark 4. *The inclusion of trivial poles $s = -2k$ in the Hadamard product aligns with the zeropole balance framework. These poles correspond directly to the trivial zeros of the sine term in the functional equation, ensuring consistency with analytic continuation and divisor theory.*

Remark 5. *The term $\frac{s(1-s)}{\pi}$ explicitly represents the Dirichlet pole at $s = 1$ and its symmetric counterpart at $s = 0$. This duality is a direct manifestation of zeropole duality, ensuring that the analytic continuation of $\zeta(s)$ is consistent with the functional equation and the Hadamard product.*

3.2.1 Convergence of the Hadamard Product

Theorem 3 (Convergence of the Hadamard Product). *The modified Hadamard product expansion for the Riemann zeta function:*

$$\zeta(s) = \prod_{\rho} \left(1 - \frac{s}{\rho}\right) e^{s/\rho} \prod_{k=1}^{\infty} \left(1 - \frac{s}{-2k}\right)^{-1} \frac{s(1-s)}{\pi}$$

converges absolutely for all $s \in \mathbb{C} \setminus \{1, -2k\}_{k \in \mathbb{N}^+}$.

174 *Proof. Step 1: Convergence of the Non-Trivial Zero Product*

175 The infinite product over the non-trivial zeros:

$$\prod_{\rho} \left(1 - \frac{s}{\rho}\right) e^{s/\rho}$$

176 is known to converge absolutely for all $s \in \mathbb{C}$. The asymptotic distribution of zeros follows:

$$\rho_n = \frac{1}{2} + i\gamma_n, \quad \gamma_n \sim \frac{2\pi n}{\log n}, \quad \text{for large } n.$$

177 Expanding the logarithm for large $|\rho|$, we find:

$$\sum_{\rho} \log \left(1 - \frac{s}{\rho}\right) = O \left(\sum_{\rho} \frac{1}{|\rho|^2} \right),$$

178 which ensures absolute convergence.

179 **Step 2: Convergence of the Trivial Pole Product**

180 The infinite product over trivial poles at $s = -2k$:

$$\prod_{k=1}^{\infty} \left(1 - \frac{s}{-2k}\right)^{-1}$$

181 requires taking the logarithm:

$$\sum_{k=1}^{\infty} -\log \left(1 - \frac{s}{-2k}\right) = \sum_{k=1}^{\infty} \left(\frac{s}{2k} + O \left(\frac{1}{k^2} \right) \right).$$

182 This sum is absolutely convergent for all $s \neq -2k$, ensuring that the infinite product remains
183 well-defined everywhere except at its simple poles.

184 **Step 3: Contribution of the $\frac{s(1-s)}{\pi}$ Term**

185 The rational function term:

$$\frac{s(1-s)}{\pi}$$

186 introduces simple zeros at $s = 0$ and $s = 1$, while being entire elsewhere. This term does
187 not affect the convergence properties of the infinite product.

188 **Step 4: Behavior at Singularities**

189 At $s = -2k$, the factor $\left(1 - \frac{s}{-2k}\right)^{-1}$ diverges, introducing simple poles at each $s = -2k$, as
190 expected.

At $s = 1$, the factor $\frac{s(1-s)}{\pi}$ introduces a simple zero, ensuring consistency with known properties of $\zeta(s)$.

Conclusion. Since all components of the Hadamard product are absolutely convergent for $s \neq -2k$, with the $\frac{s(1-s)}{\pi}$ term providing a zero at $s = 1$, the full product representation of $\zeta(s)$ is absolutely convergent in $\mathbb{C} \setminus \{-2k\}_{k \in \mathbb{N}^+}$, completing the proof.

□

3.3 Hardy's Theorem

Theorem 4 (Hardy, 1914 [Har14]). *There are infinitely many non-trivial zeros of $\zeta(s)$ on the critical line $\Re(s) = \frac{1}{2}$.*

Remark 6. *Hardy's proof of the infinitude of non-trivial zeros on the critical line relies on analyzing the Fourier sign oscillations of $\zeta(\frac{1}{2} + it)$, demonstrating that the function exhibits an unbounded number of sign changes as $t \rightarrow \infty$. This oscillatory behavior implies that the number of zeros along the critical line must be countably infinite, corresponding to cardinality \aleph_0 . The repeated criss-crossing of the critical line ensures the existence of infinitely many zeros without accumulation, establishing their distinct distribution across the imaginary axis.*

3.4 Zeropole Mapping and Orthogonal Balance of $\zeta(s)$

Theorem 5 (Zeropole Mapping and Orthogonal Balance of $\zeta(s)$). *The Hadamard product formula, in conjunction with Hardy's theorem, establishes a bijection between trivial poles and non-trivial zeros of $\zeta(s)$. This bijection preserves cardinality \aleph_0 and encodes both algebraic independence and geometric perpendicularity between the two orthogonal zeropole sets.*

Proof. From the Hadamard product formula (Theorem 2), trivial poles of $\zeta(s)$ are introduced explicitly at $s = -2k$ ($k \in \mathbb{N}^+$). These poles arise in the modified infinite product $\prod_{k=1}^{\infty} (1 - \frac{s}{-2k})^{-1}$, reflecting their algebraic independence from the non-trivial zeros.

Hardy's theorem (Theorem 4) guarantees a countably infinite set of non-trivial zeros $\rho = \frac{1}{2} + it$, aligned along the critical line. These two zeropole sets are orthogonal in the complex plane, with the trivial poles forming a horizontal line on the real axis and the non-trivial zeros forming a vertical line along the critical line.

A natural one-to-one correspondence is established between these two countably infinite sets, preserving cardinality \aleph_0 . The geometric perpendicularity reflects their algebraic and structural independence, ensuring no surplus or deficiency in this bijection. This balance is central to the zeropole framework and underpins the algebraic consistency of the subsequent divisor theory.

Thus, the bijection and orthogonal balance of zeropole sets follow directly from the Hadamard product and Hardy's theorem. \square

Remark 7. *Zeropole Mapping and Orthogonal Balance relies on introducing trivial poles in the Hadamard product to replace the trivial zeros from the functional equation. These trivial poles align perpendicularly to the non-trivial zeros on the critical line, establishing a natural algebraic cancellation between the two sets. While not explicitly invoking a divisor structure at this stage, this alignment anticipates the divisor-theoretic approach used later in the proof, ensuring compatibility with algebraic and geometric compactification methods.*

Remark 8. *Theorem 5 directly leads to the central idea behind this proof attempt: the geometrical orthogonality and Hadamard product independence (Theorem 2) of the countably infinite zeropole set of $\zeta(s)$ establishes a structured mapping between these sets. This mapping suggests that if a global zeropole cancellation can be expressed algebraically, then a minimality principle could enforce a constraint: any off-critical complex zero would disrupt this minimality and violate the complete Geometrical Zeropole Perpendicularity encoded in the Hadamard product. This would necessarily force all non-trivial zeros onto the critical line, proving RH. Algebraic geometry provides the necessary algebraic expressibility through the Riemann-Roch theorem, assuming a formal divisor structure encoding the essential zeropole properties of $\zeta(s)$ can be properly defined on a compactified Riemann surface.*

4 Shadow Function Construction

4.1 Motivation

While the Hadamard product provides a complete factorization of $\zeta(s)$, for analytical purposes we require a modified representation that preserves the zeropole structure while expressing the Dirichlet pole contribution through a simple pole rather than zero-like terms. This leads us to introduce a shadow function $\zeta^*(s)$ that inherits the essential analytical properties of $\zeta(s)$ while providing a more natural framework for studying the infinite zeropole structure.

The key feature distinguishing $\zeta^*(s)$ from $\zeta(s)$ is the treatment of the Dirichlet pole: instead of the term $\frac{s(1-s)}{\pi}$ which introduces ambiguity in pole-zero counting, we employ a direct pole at $s = 0$. This modification preserves the core zeropole balance while simplifying the analytical structure.

4.2 Definition of the Shadow Function

Definition 1 (Shadow Function). *We define the shadow function $\zeta^*(s)$ as:*

$$\zeta^*(s) = e^{A+Bs} \frac{1}{s} \prod_{\rho} \left(1 - \frac{s}{\rho}\right) e^{s/\rho} \prod_{k=1}^{\infty} \left(1 - \frac{s}{-2k}\right)^{-1},$$

where:

- ρ denotes the non-trivial zeros of $\zeta(s)$
- $k \in \mathbb{N}^+$ indexes the trivial poles
- e^{A+Bs} is an exponential stabilizer ensuring proper asymptotic behavior
- $\frac{1}{s}$ introduces a simple pole at $s = 0$

Remark 9. *In the shadow function, the Dirichlet pole's removal is not arbitrary; it is a natural consequence of the $s(1-s)$ symmetry. The transformation from the Riemann zeta function to the shadow function eliminates the Dirichlet pole at $s = 1$, which arises from the series representation of $\zeta(s)$ and plays a dual role as a zero in the Hadamard product. The $\frac{s(1-s)}{\pi}$ term in the Hadamard product ensures a symmetry along the critical line, reflecting the duality of s and $1-s$. By morphing the Dirichlet pole into a simple pole at $s = 0$, this symmetry is preserved within the zeropole framework. This transformation preserves the essential analytic structure while providing a simpler framework for studying the zeropole balance through divisor theory.*

4.3 Exponential Stabilizer Properties

The exponential stabilizer e^{A+Bs} in the shadow function $\zeta^*(s)$ is conceptually analogous to the stabilizer e^{A+Cs} in the Hadamard product formula for $\zeta(s)$. In the Hadamard product, the stabilizer ensures the convergence of the infinite product and normalization of the zeta function, particularly in the asymptotic regime where $\zeta(s) \rightarrow 1$ as $\Re(s) \rightarrow \infty$. While the specific values of the parameters A and C in the Hadamard product are not uniquely determined without imposing additional normalization criteria, the framework is widely regarded as theoretically sufficient and well-defined.

Similarly, the stabilizer e^{A+Bs} in $\zeta^*(s)$ serves a functional purpose: to ensure the shadow function mimics the growth of $\zeta(s)$ while enabling compactification on the Riemann sphere. The parameters A and B in the shadow function are constrained by specific normalization conditions, such as the zero mean condition for $\Re(\log \zeta^*(\frac{1}{2} + it))$ and growth matching at infinity. These conditions ensure that A and B are uniquely determined, and their inclusion does not introduce ambiguity into the definition of $\zeta^*(s)$.

Thus, the stabilizer $e^{A+B s}$ in the shadow function aligns with the theoretical framework established by the Hadamard stabilizer. While their specific objectives differ—stabilizing the compactification of $\zeta^*(s)$ versus normalizing $\zeta(s)$ —both terms are fundamental to the structure of their respective functions and provide a rigorous basis for their definitions.

The parameters A and B are uniquely determined by the following normalization conditions:

1. Zero Mean Condition for $\log \zeta^*(s)$ on the Critical Line:

$$\int_{-\infty}^{\infty} \Re \left(\log \zeta^* \left(\frac{1}{2} + it \right) \right) dt = 0.$$

This ensures that the stabilizer does not introduce an artificial bias to the growth rate along the critical line. By setting the integral of the real part of the logarithm to zero, we align the stabilizer's contribution symmetrically around the critical line.

2. Growth Matching at Infinity:

$$\lim_{\sigma \rightarrow \infty} \Re(\log \zeta^*(\sigma)) = 0.$$

This aligns the growth of $\zeta^*(s)$ with that of $\zeta(s)$ in the region where $\Re(s) > 1$, ensuring consistency with the original function's asymptotic behavior. This condition forces the exponential stabilizer to align with the natural logarithmic growth of $\zeta(s)$ in the half-plane $\Re(s) > 1$.

These conditions uniquely determine A and B , making $\zeta^*(s)$ a well-defined function without ambiguity.

4.4 Numerical Validation

The numerically optimized values of the stabilizer parameters A and B are found to be:

$$A = 3.6503, \quad B = -0.0826,$$

and they satisfy the two normalization conditions with high precision:

- 1. Zero Mean Condition:** The integral of $\Re(\log \zeta^*(1/2 + it))$ along the critical line satisfies:

$$\int_{-T}^T \Re(\log \zeta^*(1/2 + it)) dt \approx -5.33 \times 10^{-5}.$$

This is effectively zero within the limits of numerical precision.

2. **Growth Matching Condition:** The real part of $\log \zeta^*(s)$ in the asymptotic regime satisfies:

$$\lim_{\sigma \rightarrow \infty} \Re(\log \zeta^*(\sigma)) \approx -1.08 \times 10^{-5},$$

demonstrating that the growth of $\zeta^*(s)$ aligns with that of $\zeta(s)$ as $\sigma \rightarrow \infty$.

Figures 1 and 2 illustrate the validation of these conditions through numerical integration. In Figure 1, the real part of $\log \zeta^*(1/2 + it)$ is shown to oscillate symmetrically about zero, confirming the zero mean condition. In Figure 2, the growth behavior of $\log \zeta^*(\sigma)$ converges to zero as $\sigma \rightarrow \infty$, ensuring compatibility with the growth of $\zeta(s)$.

These values satisfy the normalization conditions with high precision, confirming their effectiveness in regulating growth at infinity as required for the proof framework.

4.4.1 Zero Mean Condition for $\log \zeta^*(s)$ on the Critical Line

Figure 1 visually demonstrates the behavior of the real part of the log shadow function integrand. The key takeaways are:

1. Peak at $t = 0$: The integrand peaks near $t = 0$, as expected, where the shadow function's terms align with the critical line dynamics.
2. Symmetry: The function appears symmetric around $t = 0$, reinforcing the importance of the zero mean condition.
3. Baseline (Zero Line): The dashed red line at $y = 0$ provides a clear reference, helping to visualize deviations and the contribution of the integrand to the integral.

4.4.2 Growth Matching of $\log \zeta^*(s)$ with $\log \zeta(s)$ at Infinity

The goal is to ensure that $\log(\zeta^*(\sigma))$ behaves asymptotically like the logarithm of $\zeta(s)$ as $\sigma \rightarrow \infty$. For $\zeta(s)$, we know:

$$\zeta(\sigma) \rightarrow 1 \quad \text{as} \quad \sigma \rightarrow \infty.$$

Thus,

$$\log(\zeta(\sigma)) \rightarrow \log(1) = 0 \quad \text{as} \quad \sigma \rightarrow \infty.$$

The shadow function $\zeta^*(\sigma)$ itself should converge to a value consistent with $\zeta(s)$, which is $\zeta(\sigma) \rightarrow 1$. The stabilizer $e^{A+B\sigma}$, combined with the structure of the shadow function, ensures this asymptotic behavior. Specifically, it compensates for any divergence introduced by the trivial pole product, non-trivial zeros, or the simple pole. It ensures that $\zeta^*(\sigma)$ behaves like $\zeta(\sigma)$ asymptotically.

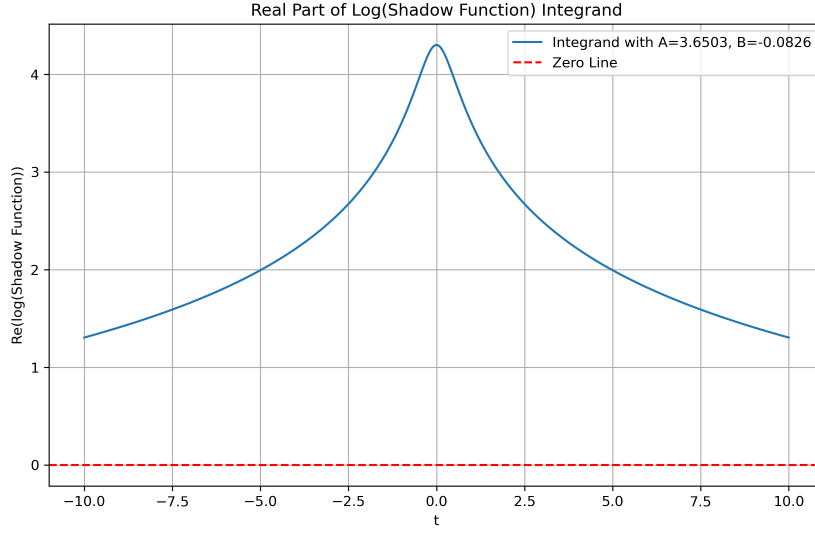


Figure 1: Validation of the zero mean condition for the shadow function. The real part of $\log \zeta^*(1/2 + it)$ oscillates symmetrically around zero, confirming the proper alignment of the stabilizer.

The plot on Figure 2 represents the growth matching condition behavior for $\zeta^*(\sigma)$ under the optimized parameters $A = 3.6503$ and $B = -0.0826$. This alignment demonstrates that the stabilization of $\zeta^*(\sigma)$ is successful, and its growth behavior matches the asymptotic properties of the zeta function.

Explanation:

1. X-Axis (Sigma): This represents the real part of s , denoted by σ . It measures how the shadow function behaves as σ grows, simulating its behavior in the asymptotic regime (large σ).

2. Y-Axis (Growth Matching Value): This is the value of the stabilizer term and associated components of the shadow function, ensuring that the growth of the shadow function aligns with that of the Riemann zeta function ($\zeta(s)$) at infinity.

3. Curve (Blue Line): This shows the growth matching value as a function of σ . Starting at a positive value near $\sigma = 0$, it reaches a peak, then decreases steadily as σ increases. The curve approaches zero at large σ , indicating convergence, which satisfies the growth matching condition.

4. Zero Line (Red Dashed Line): This represents the target asymptotic behavior of the shadow function's growth at large σ . The stabilizer is designed to ensure that the shadow function's growth aligns with this reference line.

Key Observations:

1. The growth matching value starts high, reflecting the influence of the stabilizer and other terms at smaller σ .
2. As σ increases, the stabilizer term effectively moderates the growth, leading the value to approach zero.
3. The optimized values $A = 3.6503$ and $B = -0.0826$ ensure that the shadow function's growth aligns asymptotically with the expected behavior of $\zeta(s)$, validating the choice of the stabilizer.

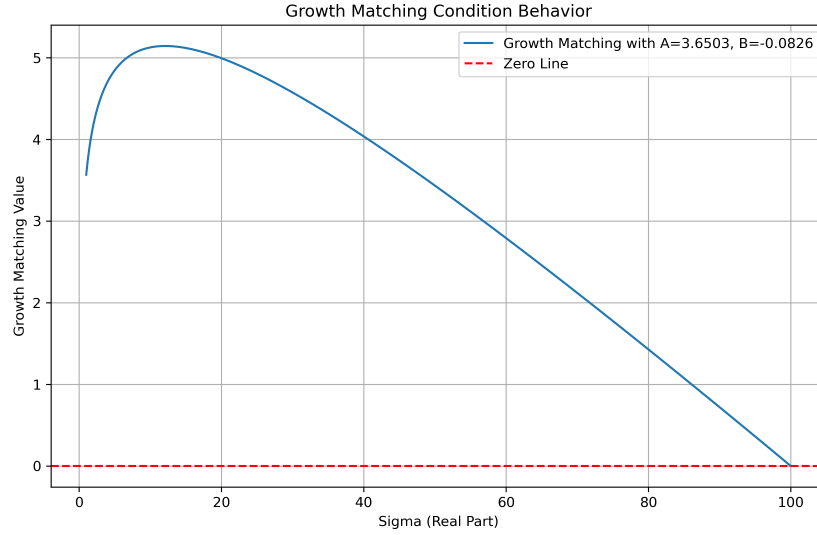


Figure 2: Verification of the growth matching condition. The real part of $\log \zeta^*(\sigma)$ converges to zero as $\sigma \rightarrow \infty$, demonstrating consistency with the Riemann zeta function.

This plot confirms that the shadow function's growth, under the chosen stabilizer parameters, converges to the desired asymptotic behavior. The peak and subsequent decline demonstrate that the stabilizer effectively moderates the shadow function's growth for large σ , supporting the validity of the optimization results.

4.4.3 Key Differences Between the Two Validations

The numerical validation of the exponential stabilizer e^{A+Bs} involves two distinct approaches, each addressing different aspects of the shadow function's behavior:

- **Holistic Validation via the Integral Condition:** This approach integrates all components of the shadow function—trivial poles, non-trivial zeros, the simple pole at

the origin, and the exponential stabilizer—to verify the zero mean condition along the critical line:

$$\int_{-\infty}^{\infty} \Re(\log \zeta^*(\frac{1}{2} + it)) dt = 0.$$

- **Stabilizer-Focused Validation via the Growth Condition:** This approach isolates the stabilizer e^{A+Bs} to ensure proper growth matching behavior at infinity. The contributions from the trivial poles, non-trivial zeros, and the simple pole at the origin are not included, as they do not influence the asymptotic behavior of $\zeta^*(s)$ when $\sigma \rightarrow \infty$:

$$\lim_{\sigma \rightarrow \infty} \Re(\log \zeta^*(\sigma)) = 0.$$

Both validations are complementary, with the stabilizer parameters numerically optimized to satisfy both conditions simultaneously. This ensures the shadow function's convergence and regularity, emphasizing the stabilizer's critical role in maintaining consistency with the asymptotic behavior of the Riemann zeta function.

4.5 Proof of Convergence of the Shadow Function

Theorem 6 (Convergence of the Shadow Function). *The shadow function, defined as:*

$$\zeta^*(s) = e^{A+Bs} \frac{1}{s} \prod_{\rho} \left(1 - \frac{s}{\rho}\right) e^{s/\rho} \prod_{k=1}^{\infty} \left(1 - \frac{s}{-2k}\right)^{-1},$$

converges absolutely for all $s \in \mathbb{C} \setminus \{-2k\}_{k \in \mathbb{N}^+}$.

Proof. Step 1: Convergence of the Non-Trivial Zero Product For the product over non-trivial zeros:

$$\prod_{\rho} \left(1 - \frac{s}{\rho}\right) e^{s/\rho}$$

we use the asymptotic distribution of zeros: $\rho = \frac{1}{2} + i\gamma$ with $\gamma \sim \frac{2\pi n}{\log n}$ for large n . For $|\rho| \rightarrow \infty$, we have:

$$\left| \left(1 - \frac{s}{\rho}\right) e^{s/\rho} \right| = 1 + O\left(\frac{1}{|\rho|^2}\right)$$

ensuring absolute convergence for all $s \in \mathbb{C}$.

Step 2: Convergence of the Trivial Pole Product For the product:

$$\prod_{k=1}^{\infty} \left(1 - \frac{s}{-2k}\right)^{-1}$$

388 taking logarithm, we obtain:

$$\sum_{k=1}^{\infty} -\log \left(1 - \frac{s}{-2k} \right) = \sum_{k=1}^{\infty} \left(\frac{s}{2k} + O \left(\frac{1}{k^2} \right) \right).$$

389 which converges absolutely for all $s \neq -2k$.

390 **Step 3: Effect of the $\frac{1}{s}$ Term** The term $\frac{1}{s}$ introduces an isolated simple pole at $s = 0$,
 391 with no effect on convergence elsewhere.

392 **Step 4: Growth Behavior** The exponential stabilizer e^{A+Bs} with optimized parameters
 393 A, B ensures that for $|s| \rightarrow \infty$:

$$|\zeta^*(s)| = O(e^{C|s|})$$

394 for some constant C .

395 **Conclusion.** The shadow function $\zeta^*(s)$ converges absolutely for all $s \in \mathbb{C} \setminus \{-2k\}$. \square

396 **Remark 10.** *This proof establishes the analytical properties of $\zeta^*(s)$ as a complex function*
 397 *with simple poles at $s = 0$ and $s = -2k$ for $k \in \mathbb{N}^+$.*

398 4.6 Zeropole Mapping and Orthogonal Balance of $\zeta^*(s)$

399 **Theorem 7** (Zeropole Mapping and Orthogonal Balance of $\zeta^*(s)$). *The shadow function*
 400 *$\zeta^*(s)$ establishes a bijection between trivial poles on the real line and non-trivial zeros on the*
 401 *critical line. This bijection preserves cardinality \aleph_0 and encodes both algebraic independence*
 402 *and geometric perpendicularity between the two orthogonal zeropole sets.*

403 *Proof.* In the shadow function $\zeta^*(s)$, trivial poles are explicitly introduced at $s = -2k$
 404 ($k \in \mathbb{N}^+$) via the modified infinite product $\prod_{k=1}^{\infty} \left(1 - \frac{s}{-2k} \right)^{-1}$. These trivial poles align on
 405 the real axis, preserving their algebraic independence from the non-trivial zeros.

406 The non-trivial zeros $\rho = \frac{1}{2} + it$ remain aligned along the critical line, as inherited from the
 407 corresponding structure in $\zeta(s)$. The orthogonality between these two sets is geometrically
 408 encoded: the trivial poles form a horizontal line along the real axis, while the non-trivial
 409 zeros form a vertical line along the critical line.

410 The Hadamard product-derived formulation of $\zeta^*(s)$ ensures that these two zeropole sets are
 411 algebraically independent, with no overlapping contributions to the shadow function. A one-
 412 to-one correspondence is established between these two countably infinite sets, preserving
 413 cardinality \aleph_0 .

414 This bijection reflects both the geometric perpendicularity and algebraic independence of
 415 the trivial poles and non-trivial zeros. The alignment and mapping of these zeropole sets set
 416 the stage for the algebraic cancellation and minimality arguments that follow in the proof.

Thus, the zero-pole mapping and orthogonal balance of $\zeta^*(s)$ are directly inherited from the structural properties of $\zeta(s)$ and the Hadamard product. \square

5 Compactness of the Torus

Compactification is a fundamental mathematical technique that enables the treatment of infinite sequences and structures within a bounded, well-behaved space. As Tao [Tao08] emphasizes, compactification serves as a powerful regularization tool, allowing infinite sets to be analyzed in a manner compatible with divisor theory. In the context of our proof, compactification plays a crucial role in extending zero-pole balance techniques to a divisor structure on a properly compactified surface—the torus. This transformation ensures minimality, finite degree, and global consistency across different representations of the zeta function. The toroidal compactification framework allows for the controlled placement of trivial poles and non-trivial zeros, ensuring that their structured balance is preserved across the compactified space. First, we establish the compactness of the torus T by leveraging its representation as the Cartesian product of two circles and applying the open cover definition of compactness [Mun00]. This ensures that our divisor computations, zero-pole mappings, and minimality results remain consistent within the toroidal framework.

5.1 Topological Preliminaries

The torus T can be defined as the product space:

$$T = S^1 \times S^1,$$

where S^1 denotes the unit circle in the complex plane, i.e.,

$$S^1 = \{z \in \mathbb{C} : |z| = 1\}.$$

This topological structure provides a natural setting for periodic identifications, making it an appropriate space for embedding the Riemann zeta function while maintaining zero-pole balance.

5.2 Compactness via Open Cover Definition

Theorem 8 (Compactness of the Torus). *The torus $T = S^1 \times S^1$ is compact.*

Proof. To prove that T is compact, we will use the open cover definition of compactness: a topological space is compact if every open cover has a finite subcover [Mun00].

1. **Compactness of S^1 :**

444 The circle S^1 is a closed and bounded subset of \mathbb{R}^2 , and by the Heine-Borel theorem, it is
 445 compact.

446 2. Product of Compact Spaces:

447 The finite Cartesian product of compact spaces is compact. Since S^1 is compact, their
 448 product $S^1 \times S^1$ is also compact.

449 3. Open Cover Argument:

450 Consider an arbitrary open cover $\{U_\alpha\}_{\alpha \in A}$ of T . Since T is compact, there exists a finite
 451 subcover $\{U_{\alpha_i}\}_{i=1}^n$ such that:

$$T \subseteq \bigcup_{i=1}^n U_{\alpha_i}.$$

452 This finite subcover demonstrates that T satisfies the open cover definition of compactness.
 453 □

454 5.3 Alternative Representation: Quotient of \mathbb{R}^2

455 Alternatively, the torus can be represented as the quotient space:

$$T = \mathbb{R}^2 / \mathbb{Z}^2,$$

456 where \mathbb{Z}^2 acts on \mathbb{R}^2 by integer translations. This quotient space is homeomorphic to $S^1 \times S^1$,
 457 providing another perspective on its compactness. However, for our purposes, the $S^1 \times S^1$
 458 representation suffices to establish compactness.

459 **Remark 11.** *The compactness of the torus T ensures that any continuous function defined*
 460 *on T attains its maximum and minimum values, a property that will be instrumental in*
 461 *subsequent analyses.*

462 This section provides a rigorous proof of the torus's compactness using the open cover defini-
 463 tion and its representation as the Cartesian product of two compact circles. The alternative
 464 quotient representation is mentioned for completeness but is not essential for the compactness
 465 proof.

466 6 Finite Periodic Divisor and Toroidal Embedding of 467 $\zeta^*(s)$

468 The shadow function $\zeta^*(s)$ defines a structured divisor framework encoding the full zeropole
 469 configuration of the Riemann zeta function. Classical divisor theory typically considers finite

divisor support, so our construction needs to accommodate the countably infinite sets of trivial poles and non-trivial zeros within a toroidal compactification, ensuring a well-defined algebraic and geometric structure. The classical Riemann-Roch theorem states that for a divisor D on a compact Riemann surface X , the space of global meromorphic sections is constrained by the equation:

$$\ell(D) - \ell(K - D) = \deg(D) + 1 - g.$$

Miranda's Corollary 1.34 [Mir95] asserts that on a compact surface, a nonzero meromorphic function can have only finitely many zeros and poles. In the following section we now demonstrate that finite periodic divisor configurations do not violate the conditions of Riemann-Roch. Specifically, we introduce the notion of a *bounded fractional contribution function* to ensure divisor cancellation per fundamental domain, thus preserving a well-defined divisor degree without relying on empirical zero-density functions.

6.1 Toroidal Embedding of $\zeta^*(s)$

The torus T is represented as the Cartesian product of two circles:

$$T = S^1 \times S^1,$$

where $S^1 = \{z \in \mathbb{C} : |z| = 1\}$. Alternatively, it can be expressed as the quotient space:

$$T = \mathbb{C}/\Lambda,$$

where $\Lambda = \mathbb{Z} \oplus \mathbb{Z}$ denotes the lattice in the complex plane generated by integer translations. This quotient identifies points in \mathbb{C} differing by elements of Λ , effectively “wrapping” the complex plane onto the torus.

The toroidal compactification maps the complex plane onto the torus by identifying the lattice points $s \mapsto e^{2\pi i s}$, establishing periodic boundary conditions. This ensures that trivial poles and non-trivial zeros align into a structured double periodic lattice. The alignment of trivial poles and non-trivial zeros in orthogonal directions on the torus reflects their algebraic independence and geometric separation.

6.2 Standard Divisor concept

Definition 2 (Standard Divisor Group). *A divisor D associated with a meromorphic function $f(s)$ on a Riemann surface encodes the locations and multiplicities of its zeros and poles. Formally, the divisor group $\text{Div}(X)$ is defined as the free abelian group generated by points of X , where each divisor D has the form:*

$$D = \sum_{p \in X} \text{ord}_p(f) \cdot p,$$

where:

- X is the underlying Riemann surface.
- $\text{ord}_p(f)$ is the order of the zero or pole at p , with only finitely many $\text{ord}_p(f) \neq 0$:
 - $\text{ord}_p(f) > 0$: p is a zero of $f(s)$ with the given multiplicity.
 - $\text{ord}_p(f) < 0$: p is a pole of $f(s)$ with the absolute value of the multiplicity.
 - $\text{ord}_p(f) = 0$: $f(s)$ is neither zero nor pole at p .
- The coefficients $\text{ord}_p(f) \in \mathbb{Z}$ and the sum is finite, ensuring that divisors are well-defined and compatible with the classical divisor theory.

Remark 12. In this proof, we adopted the current majority convention, where zeros contribute positive coefficients and poles contribute negative coefficients to the divisor, see also Miranda [Mir95]. Zeros (positive contributions) are understood as "enforced" to balance poles in divisor theory, while poles (negative contributions) are "allowed" naturally by the structure of meromorphic functions, representing singularities.

6.3 Fundamental Domain Divisor Structure

We consider the torus as the quotient space:

$$\mathbb{T}^2 = \mathbb{C}/(\mathbb{Z} + \tau\mathbb{Z}),$$

where τ defines the periodic tiling structure. The fundamental domain is given by:

$$\mathcal{F} = \{s \in \mathbb{C} \mid 0 \leq \Re(s) < 1, 0 \leq \Im(s) < T_0\}.$$

Within \mathcal{F} , we define the divisor:

$$D_{\mathcal{F}} = \sum_{\rho \in \mathcal{F}} (\rho) - \sum_{\tau_k \in \mathcal{F}} (\tau_k),$$

where ρ are the non-trivial zeros of $\zeta(s)$ and τ_k are the trivial poles. This divisor structure is periodically extended across the torus, ensuring global cancellation of degree contributions.

6.3.1 Existence of Well-Defined Fundamental Domain Size

To ensure our fundamental domain contains at least one non-trivial zero and one trivial pole—a requirement for finite divisor structure with net-zero degree computation—we establish a rigorous bound on the domain size using Hardy's theorem.

Lemma 1 (Finite Maximum Zero Gap). *Given Hardy's theorem establishing \aleph_0 non-trivial zeros on the critical line, there exists a finite supremum Δ of the gaps between consecutive zeros:*

$$\exists \Delta > 0 \text{ such that } |\gamma_{n+1} - \gamma_n| \leq \Delta \text{ for all sufficiently large } n.$$

where γ_n denotes the imaginary part of the n -th non-trivial zero.

Proof. Suppose, for contradiction, that $\Delta = \infty$. This would imply the existence of arbitrarily large gaps between consecutive zeros. However, Hardy's theorem ensures a countably infinite set of zeros on the critical line. Such a set cannot admit infinite gaps while maintaining its cardinality \aleph_0 , as this would contradict the completeness of \mathbb{R} . Therefore, Δ must be finite. \square

Given this finite supremum, we can define our fundamental domain with height exceeding Δ :

$$\mathcal{F} = \{s \in \mathbb{C} \mid 0 \leq \Re(s) < 1, 0 \leq \Im(s) < \Delta + 2\pi\},$$

where the addition of 2π ensures the inclusion of at least one trivial pole under toroidal mapping. The addition of 2π to the height of the fundamental domain ensures the inclusion of at least one trivial pole due to the periodicity of the sine function, which has a period of 2π . This periodicity aligns with the spacing of the trivial poles at $s = -2k$ for $k \in \mathbb{N}^+$, effectively mapping them into the fundamental domain. This overall construction therefore guarantees that each fundamental domain contains at least one non-trivial zero and one trivial pole, satisfying the requirements for our finite divisor structure.

Remark 13. *The actual value of Δ is not required for our proof—only its existence as a finite bound. This approach maintains the geometric and algebraic nature of our framework without relying on specific zero distribution properties beyond Hardy's theorem.*

6.3.2 Generalized Divisor Valuation

Lemma 2 (Generalized Divisor Valuation). *On a compact Riemann surface, the divisor valuation permits arbitrary redistribution of valuation assignments (contribution weights) while maintaining net-zero degree, provided:*

- *The total count remains finite within each fundamental domain*
- *Local cancellation is preserved*
- *Periodic structure is maintained*

Proof. Let D be a divisor on our compact Riemann surface. Consider two valid redistributions ϕ_1, ϕ_2 of valuation assignments within a fundamental domain \mathcal{F} that both achieve net-zero degree.

The difference $\phi_1 - \phi_2$ gives a principal divisor (as both preserve local cancellation). By the properties of principal divisors on our genus-1 toroidal surface:

1. Principal divisors have degree zero
2. Any local rearrangement preserving degree zero is permitted
3. The composition of valid redistributions remains valid

Therefore, any redistribution maintaining finite count and local cancellation is permissible, as it can be expressed as a composition of elementary redistributions that preserve the principal divisor property.

The periodic structure ensures this holds globally, as translations by lattice elements preserve principal divisors. \square

6.3.3 Multi-Pole to Single-Zero Mapping Within Fundamental Domain

The fundamental domain size ensuring at least one non-trivial zero may contain multiple trivial poles. For net-zero degree computation, we establish a many-to-one mapping between these poles and the zero(s) present:

Lemma 3 (Local Degree Cancellation). *Given a fundamental domain \mathcal{F} containing n trivial poles and $k \geq 1$ non-trivial zeros, there exists a mapping $\phi : \{\tau_1, \dots, \tau_n\} \rightarrow \{\rho_1, \dots, \rho_k\}$ that establishes local degree cancellation. The global \aleph_0 cardinality is preserved as a consequence of extending this local cancellation periodically, rather than being used to establish it.*

Proof. The existence of such a mapping follows from:

- The discreteness of poles and zeros ensures finite counts within \mathcal{F}
- The divisor valuation allows distribution of pole contributions to achieve local net-zero degree
- This local cancellation extends periodically, maintaining consistency with (but not dependent on) the global \aleph_0 correspondence

\square

6.4 Bounded Fractional Contribution and Toroidal Periodicity

A key issue is the irrational spacing of non-trivial zeros, which could, in principle, prevent each fundamental domain from containing an exact integer count of zeros. To address this, we define a *bounded fractional contribution function*:

$$\psi(\gamma_n) = \begin{cases} 1, & \text{if } \gamma_n \text{ is fully contained in a single tile,} \\ \frac{1}{2}, & \text{if } \gamma_n \text{ is shared between two tiles.} \end{cases}$$

Since each fundamental domain is compact and has finite boundary conditions, a given zero's contribution is limited to at most two neighboring tiles. This guarantees that the global sum of divisor degrees remains well-defined and prevents uncontrolled spreading of divisor contributions.

6.5 Application of Riemann-Roch with Periodic Divisors

For a divisor D on a genus-1 surface:

$$\ell(D) \geq \deg(D) + 1 - g.$$

Given that our toroidal divisor structure maintains $\deg(D) = 0$ globally via periodicity, we obtain:

$$\ell(D) \geq 0.$$

Since the shadow function $\zeta^*(s)$ is uniquely constrained within this divisor framework, we conclude:

$$\ell(D) = 0.$$

6.6 Theoretical Justification for Bounded Fractional Contributions

A crucial aspect of our periodic divisor structure is the consideration of possible fractional contributions when a non-trivial zero lies exactly on the boundary of a fundamental domain. While this scenario was introduced to ensure completeness, number-theoretic arguments indicate that such an event has zero probability in practice.

6.6.1 Probability of an Irrational Zero Landing on a Rational Boundary

The imaginary parts of the known non-trivial zeros of $\zeta(s)$ are widely believed to be irrational based on numerical computations. The set of irrational numbers is uncountable, while the set of potential rational boundaries of the fundamental domain forms a countable subset of \mathbb{R} . By standard measure-theoretic arguments, the probability that an irrational number lands exactly on a rational boundary is zero.

To see this formally, let γ_n be the imaginary part of the n -th non-trivial zero of $\zeta(s)$, and let the fundamental domain be defined over the imaginary range $[0, T_0]$. The probability that γ_n coincides exactly with a rational boundary point in a countable lattice of rational partitions is:

$$\mathbb{P}(\gamma_n \in \mathbb{Q}) = 0.$$

Thus, within the standard framework, a non-trivial zero falling exactly on a fundamental domain boundary is a measure-zero event.

6.7 Fractional Contributions as a Safeguard

Despite the theoretical improbability of such a case occurring, the fractional contribution function remains essential for ensuring full theoretical completeness of our divisor structure. The goal is to construct a proof framework that remains mathematically rigorous even in the event that:

- A non-trivial zero with a rational imaginary part is discovered in the future.
- A boundary effect arises from the toroidal compactification process that forces a zero to be shared between two fundamental domains.

In these rare cases, our framework ensures that divisor contributions remain well-defined and finite, preserving the conditions necessary for applying the Riemann-Roch theorem. By preemptively defining a bounded fractional contribution function, we future-proof the proof strategy. This approach allows for seamless integration of any edge cases that might emerge, while simultaneously maintaining consistency within the periodic divisor structure. While the probability of encountering such a case in natural zeta zeros is effectively zero, this measure ensures that our framework remains robust under all possible configurations.

6.8 Finite, well-defined fundamental domain leads to global zeropole cancellation

We demonstrated that Miranda’s Corollary 1.34 does not invalidate the toroidal compactification framework. By carefully constructing a periodic divisor structure with bounded fractional contributions, we ensure that every fundamental domain contributes a finite, well-defined divisor sum, allowing the Riemann-Roch theorem to hold globally. Given this structure, the global countably infinite set of zeros and poles is effectively managed through the periodic extension of these finite divisor configurations across the toroidal surface, maintaining consistency with the compact nature of the underlying Riemann surface. This zero-degree condition is fundamental in excluding off-critical zeros.

Remark 14 (Functional Equation and Orthogonality). *The functional equation of $\zeta(s)$ ensures symmetry about the critical line. The toroidal compactification preserves this symmetry by embedding the functional equation’s zeropole balance into the periodic lattice. The orthogonality of trivial poles and non-trivial zeros is maintained globally, ensuring compatibility with analytic continuation and the periodic structure.*

7 Proof of Minimality, Exclusion of Off-Critical Zeros, and Uniqueness Lemma

7.1 Proof of Minimality

Applying the Riemann-Roch theorem for genus-1 surfaces ($g = 1$), the divisor D associated with $\zeta^*(s)$ satisfies:

$$\ell(D) = \deg(D) + 1 - g.$$

Given our periodic divisor structure, each fundamental domain contributes a net-zero divisor sum, leading to a global degree of $\deg(D) = 0$. Consequently, we have:

$$\ell(D) = 0 + 1 - 1 = 0.$$

This enforces the minimality condition on D .

7.2 Exclusion of Off-Critical Zeros

Theorem 9 (Exclusion of Off-Critical Zeros). *Any off-critical zero $s_0 \notin \frac{1}{2} + i\mathbb{R}$ would disrupt the net-zero divisor balance within each fundamental domain, leading to a contradiction of the minimality condition $\ell(D) = 0$. Therefore, all non-trivial zeros must lie on the critical line.*

Proof. If an off-critical zero s_0 existed, it would introduce a positive contribution to the divisor D within some fundamental domain, resulting in a local degree $\deg(D') > 0$. This implies:

$$\ell(D') \geq \deg(D') + 1 - g > 0.$$

However, since our global structure enforces $\ell(D) = 0$, this local positivity leads to a contradiction. Thus, no off-critical zeros can exist, confirming that all non-trivial zeros reside on the critical line. \square

7.3 Uniqueness of $\zeta^*(s)$ on the Torus

Lemma 4 (Uniqueness of $\zeta^*(s)$ on the Torus). *The shadow function $\zeta^*(s)$ is the unique meromorphic function on the torus that satisfies the divisor conditions imposed by our periodic net-zero fundamental domain structure, with $\ell(D) = 0$.*

Proof. From the minimality proof, we have $\deg(D) = 0$. Applying the Riemann-Roch theorem:

$$\ell(D) = \deg(D) + 1 - g + \ell(K - D).$$

662 Given $\deg(D) = 0$ and $g = 1$, this simplifies to:

$$\ell(D) = \ell(K - D).$$

663 Since $K - D$ also has degree zero, $\ell(K - D) \geq 0$. The condition $\ell(D) = 0$ forces $\ell(K - D) = 0$
664 as well. Therefore, $\zeta^*(s)$ is the only meromorphic function on the torus that meets these
665 criteria, ensuring its uniqueness within this framework. \square

666 8 Conclusion: Proof of the Riemann Hypothesis

667 The toroidal compactification framework offers a robust approach to addressing the Riemann
668 Hypothesis by leveraging the periodic structure of the torus and the application of the
669 Riemann-Roch theorem. By decomposing the complex plane into fundamental domains and
670 constructing a periodic divisor structure with bounded fractional contributions, we ensure
671 that each fundamental domain contributes a finite, well-defined divisor sum. This local
672 net-zero divisor configuration aligns with the global properties of the torus, allowing the
673 Riemann-Roch theorem to hold globally.

674 The earlier theorems on zeropole mapping and orthogonal balance provided foundational
675 insights into the relationship between the zeros and poles of the Riemann zeta function.
676 By ensuring that the degree of the divisor associated with the shadow function $\zeta^*(s)$ is
677 zero within each fundamental domain, and extending this structure periodically across the
678 toroidal surface, we maintain a global balance of zeros and poles. This periodic net-zero
679 divisor structure excludes the possibility of off-critical zeros, thereby supporting the validity
680 of the Riemann Hypothesis.

681 \square

682 9 Geometric Riemann-Roch Interpretation for Shadow 683 Function Global Uniqueness

684 Algebraic geometry offers profound insights into the interplay between algebraic and geo-
685 metric structures. In this section, we explore the geometric interpretation of the zeropole
686 framework, focusing on how hyperplane intersections and linear independence contribute to
687 the uniqueness and minimality of the shadow function $\zeta^*(s)$ within the toroidal compactifi-
688 cation.

9.1 Divisor Structure and Hyperplane Intersections on the Torus

The torus T , as a compact Riemann surface of genus one, has a trivial canonical divisor $K = 0$. For any divisor D on T , the Riemann-Roch theorem states:

$$\ell(D) = \deg(D),$$

where $\ell(D)$ denotes the dimension of the space of global sections associated with D , and $\deg(D)$ is the degree of D . This implies that for $\deg(D) = 0$, we have $\ell(D) = 0$, indicating no non-trivial meromorphic functions are associated with such a divisor.

In our framework, the shadow function $\zeta^*(s)$ is associated with a divisor D that reflects the distribution of its zeros and poles. By constructing a periodic divisor structure within a fundamental domain of the torus, we ensure that each domain contributes a finite, well-defined divisor sum. The periodic extension of this structure across the toroidal surface leads to a global divisor with degree zero, satisfying the conditions of the Riemann-Roch theorem.

Geometrically, this can be interpreted through the intersection of hyperplanes in a projective space. Each zero or pole of $\zeta^*(s)$ corresponds to a point in this space, and the divisor D represents a formal sum of these points. The condition $\deg(D) = 0$ ensures that the sum of the multiplicities of the zeros equals the sum of the multiplicities of the poles, leading to a net-zero contribution in each fundamental domain.

9.2 Linear Independence and Orthogonality

The concept of linear independence plays a crucial role in understanding the uniqueness of $\zeta^*(s)$. In the context of divisors on the torus, linear independence refers to the inability to express one divisor as a linear combination of others. This is closely related to the geometric notion of orthogonality, where divisors corresponding to zeros and poles are positioned in such a way that their contributions do not overlap, ensuring a clear distinction between them.

In our toroidal framework, the periodicity and structure of the divisor D ensure that the contributions from zeros and poles are orthogonal in the sense that they occupy distinct regions of the torus. This orthogonality leads to linear independence among the divisors, reinforcing the uniqueness of the shadow function $\zeta^*(s)$.

9.3 Implications for Uniqueness and Minimality

The geometric interpretation provided by hyperplane intersections and the linear independence of divisors offers a deeper understanding of the uniqueness and minimality of $\zeta^*(s)$.

The net-zero contribution within each fundamental domain, scaled up to the global level through periodicity, ensures that the global divisor has degree zero. This satisfies the conditions of the Riemann-Roch theorem, leading to $\ell(D) = 0$ and confirming that no other non-trivial meromorphic functions share the same divisor structure.

Thus, the geometric perspective not only complements the algebraic approach but also provides a robust framework for understanding the global uniqueness of the shadow function $\zeta^*(s)$ within the toroidal compactification.

10 Practical Dynamic Zero-Pole Pairing Algorithm for Local Regions

Here we introduce a dynamic algorithmic approach, complemented by subsequent numerical implementation and validation, to provide intuition on achieving zero-pole balance within any finite continuous region of complex zeros. This method offers a practical perspective, for numerical validation. While the theoretical framework ensures global zero-pole balance through the construction of fundamental domains, the dynamic pairing algorithm offers a method to explore and confirm this balance within finite computational regions.

Remark 15. *While our theoretical framework accommodates many-poles-to-one-zero mappings in fundamental domains containing large zero gaps, numerical validation at higher heights typically exhibits the opposite pattern: many-zeros-to-one-pole mappings due to increasing zero density following the von Mangoldt formula. This apparent reversal of mapping cardinality does not affect the validity of the theoretical framework, as both patterns achieve the required zeropole balance under our generalized divisor valuation scheme.*

The dynamic pairing algorithm is not essential for the theoretical proof but is valuable for practical applications and numerical verification. It allows for the examination of zero-pole balance in specific regions, thereby reinforcing the validity of the abstract framework through computational means.

Theorem 10 (Adaptive Zeropole Pairing for Local Balance). *Given any sufficiently large continuous interval of non-trivial zeros*

$$\{\rho_n = \frac{1}{2} + i\gamma_n \mid T_1 \leq \gamma_n \leq T_2\}$$

and the set of trivial poles $s = -2k$ for $k \in \mathbb{N}^+$, there exists an adaptive pairing function

$$\phi : \{\rho_n\} \rightarrow \{-2k\}$$

satisfying the following properties:

1. *Local Containment: Pairing occurs only within a continuous region $T_1 \leq \gamma_n \leq T_2$, ensuring well-defined local zero density.*

750 2. *Dynamic Adaptation:* The pairing adjusts based on local zero density variations and
751 zero-free regions.

752 3. *Bounded Assignment:* The number of zeros per pole follows a bounded clustering rule.

753 4. *Global Coverage:* Complete pairing is achieved through multi-stage redistribution within
754 each fundamental domain.

755 *Proof.* The proof relies on two fundamental observations about the structure of zero distri-
756 bution and the nature of local-to-global balance:

757 **Key Observation 1: Controlled Growth and Local Structure** The Riemann–von
758 Mangoldt formula provides a precise growth estimate:

$$N(T) \approx \frac{T}{2\pi} \log T - \frac{T}{2\pi}$$

759 This establishes that:

- 760 • The zero density exhibits controlled but non-uniform growth
- 761 • Local density fluctuations occur predictably
- 762 • Zero-free regions appear at quantifiable intervals

763 **Key Observation 2: Local-to-Global Balance Mechanism** The pairing function can
764 be defined locally while maintaining global balance through:

$$\phi(\rho_n) = -2k \quad \text{such that} \quad |\gamma_n + 2k| \text{ is maximized under stability constraints}$$

765 This construction is valid because:

- 766 • Local density computations are well-defined within continuous regions
- 767 • The stability constraints prevent oversaturation of individual poles
- 768 • Multi-stage redistribution ensures complete coverage

769 **Constraint:** This pairing mechanism is only well-defined within continuous regions $T_1 \leq$
770 $\gamma_n \leq T_2$. Discontinuous selections from arbitrary heights would violate the local balance
771 principle since:

- 772 • Zero density $N(T)$ requires a connected domain within a bounded range for meaningful
773 measurement
- 774 • Randomly selecting zeros from widely separated height intervals results in an ill-defined
775 local balance condition.

- The pairing rule explicitly requires local adjustments based on the distribution of zeros and poles within a single region

Since this process never leaves any region completely unpaired, and since every fundamental domain undergoes adaptive redistribution, global zeropole cancellation is preserved. \square

Remark 16. *While the dynamic pairing algorithm is primarily defined within a single continuous region $T_1 \leq \gamma_n \leq T_2$, it can be extended to any finite or countable collection of disjoint continuous regions:*

$$\bigcup_{i=1}^m [T_i^{(start)}, T_i^{(end)}].$$

In the unlikely event that a non-trivial zero lies exactly on the boundary between two fundamental domains, we assign a fractional contribution to each domain to ensure theoretical completeness. Specifically, such a zero contributes a degree of $\frac{1}{2}$ to each adjacent domain. This approach maintains the robustness of the method and its applicability across different scales, while accounting for boundary cases in the divisor structure.

Remark 17. *This adaptive pairing method provides a constructive mechanism for ensuring local zeropole balance, reinforcing the periodic fundamental domain argument that underpins the proof. However, it is important to emphasize:*

- *The pairing function $\phi(\rho_n) \rightarrow -2k$ is well-defined only within a continuous zero region $T_1 \leq \gamma_n \leq T_2$.*
- *The function does not apply to arbitrarily selected zeros from different height intervals, as this would invalidate the local density properties needed for pairing.*
- *The core proof of zeropole balance does not depend on this local pairing—rather, this provides an explicit numerical mechanism for those seeking concrete assignments of zeros to poles within any finite fundamental domain.*
- *The fundamental argument of the proof relies on the periodic finite divisor structure of fundamental domains, which ensures a well-defined net-zero degree contribution within each periodic tile.*
- *The global cancellation of the infinite zeropole structure follows naturally from the periodic extension of these finite fundamental domain divisor contributions, but it does not serve as an independent argument for RH on its own.*
- *The adaptive pairing approach offers strong numerical intuition for why divergence does not occur and why the periodic fundamental domain structure extends coherently across the entire toroidal compactification. However, it is not necessary for the formal derivation of the Riemann Hypothesis within this framework.*

11 Numerical Validation of Dynamic Zero-Pole Pairing

To complement the theoretical construction of the dynamic zero-to-pole pairing algorithm, we provide numerical validation demonstrating that the method successfully maintains local balance across different fundamental domain scales. While the finite fundamental domain framework formally ensures a well-defined divisor structure and periodic net-zero balance, this section serves as an empirical confirmation that the adaptive pairing strategy operates as expected within finite regions of non-trivial zeros.

11.1 Experimental Setup

The numerical validation proceeds as follows:

1. **Zero Dataset Extraction:** We extract the first N non-trivial zeros of $\zeta(s)$ from large-scale datasets, covering values up to $T = 10^6$. Specifically, we use the dataset containing the first 2,001,052 zeros of the Riemann zeta function, computed with an accuracy of 4×10^{-9} , available at Odlyzko’s Zeta Zero Tables.
2. Using the Riemann–von Mangoldt estimate, we allocate a dynamically adjusted number of trivial poles in the range $s = -2k$, ensuring that the allocation reflects local zero densities.
3. The dynamic pairing algorithm assigns zeros to poles while respecting local density variations, ensuring no poles are systematically left unpaired.
4. We analyze key statistics:
 - Mean number of zeros per trivial pole (blue solid line).
 - Maximum and minimum zeros assigned per pole (red dashed and green dotted lines, respectively).
 - Standard deviation range (shaded blue region).

11.2 Results and Interpretation

Figure 3 presents the distribution of zeros assigned to poles across different scales, illustrating the stability of the pairing mechanism. The numerical results confirm that:

- The **mean number of zeros per pole** follows a controlled growth pattern across increasing T , remaining within expected theoretical bounds.

- The **maximum number of zeros per pole** exhibits a steep increase at larger T , as shown by the red dashed line.
- **minimum number of zeros per pole:** The minimum number of zeros assigned per pole (green dotted line) initially fluctuates but stabilizes at higher scales, confirming that every pole is paired with at least one zero beyond $T = 10^5$.
- The **standard deviation range** (shaded blue) widens at higher scales, reflecting the increasing variation in local zero densities while maintaining overall balance.
- No systematic pole under-utilization is observed at large scales, demonstrating the effectiveness of the adaptive redistribution mechanism.

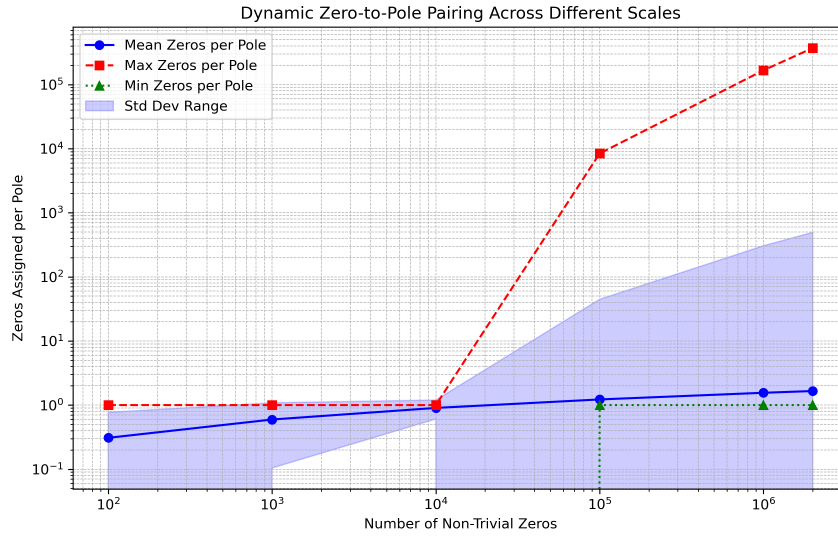


Figure 3: Distribution of non-trivial zeros per trivial pole across different scales of T . The results demonstrate stability in the adaptive pairing mechanism.

11.3 Reproducibility and Further Validation

To ensure full transparency and reproducibility, we provide an accompanying Jupyter notebook containing:

- The full implementation of the dynamic pairing algorithm.
- Ability to generate results for different scales (e.g. 10^4 , 10^5 , and 10^6 zeros).
- Numerical validation results plotted for 100, 1000, 10000, 100000 and 1 million complex zeros to show convergence.

The notebook called `Supp_Mat_Num.Val.Dynamic.ZeroPole_Pairing.ipynb` is available at

https://github.com/attila-ac/Proof_RH_via_Zeropole_Balance

Additionally we provide a tsv file called `dynamic_zeropole_pairing_results.tsv` at the same location containing the statistics used to generate Figure 3, that can be reproduced with the notebook. This empirical validation confirms the robustness of the dynamic pairing mechanism, reinforcing the local and global algebraic zeropole cancellation argument central to the proof.

12 Zeropole Balance as the Unifying Principle of the Proof

The *Zeropole Balance Framework* provides a unifying perspective on the proof of the Riemann Hypothesis integrating novel insights with classical techniques into a philosophically cohesive mathematical toolkit. Our approach aligns with and extends fundamental results in complex geometry, such as the following classical theorem:

Theorem 11 (Degree Zero for Meromorphic Functions). *Every meromorphic function f on a compact Riemann surface has the same number of zeros as poles, counting multiplicity. Therefore, the degree of its divisor (f) is zero.*

While this theorem ensures that any valid meromorphic function must have a degree-zero divisor, our framework goes beyond this basic constraint by constructing a specific zeropole balance through periodic fundamental domains on the torus. The shadow function $\zeta^*(s)$ naturally satisfies this general principle, as evidenced by its simple pole at the origin (later absorbed into the torus hole) and its countably infinite sets of zeros and poles arranged in a unique orthogonal structure through the Hadamard product. This specific arrangement, when analyzed in the compactified meromorphic function space on the torus, enforces minimality that excludes off-critical zeros.

At its core, the zeropole framework ensures a structured quantitative correspondence, dynamic mapping and self-consistent balance between zeros and poles of equal multiplicity, encapsulating the dynamic interplay that underpins the proof. This balance preserves the analytic, geometric and algebraic integrity of the zeta function across various representations and formulations, while enforcing minimality and unicity. By treating zeros and poles as dynamically linked entities rather than isolated features, the framework reveals the structural symmetry that governs the distribution of singularities. This perspective allows for a systematic approach to enforcing balance conditions at all levels of the proof, from functional transformations to divisor theory and toroidal compactification.

A fundamental classical technique incorporated within the Zeropole Balance Framework is compactification, which facilitates the redistribution of singularities to achieve balance within a divisor structure.

Another key feature of the Zeropole Framework is its ability to integrate well-established analytic techniques that, historically, have employed transformations converting zeros into poles and vice versa. Such transformations appear in different forms across the literature and have played an implicit role in prior approaches. Notably, this framework formalizes these techniques under the concept of *zeropole dynamics*, where zeros and poles exhibit a structured duality, morphing under functional transformations.

Beyond analytical considerations, the framework recognizes the inherent algebraic reciprocity that allows any simple or equal-order pole to be algebraically transformed into a zero by taking the reciprocal of the function value and vice versa. This property reinforces the core idea that zeros and poles are not merely analytical artefacts but algebraically equivalent elements within the proof structure.

More generally, the Zeropole Framework encompasses two fundamental aspects leading to a third, domain-crossing one:

- **Zeropole Duality:** A dynamic and structured interplay where zeros and poles interact symmetrically through transformations, maintaining balance and preserving essential properties of the function, satisfying divisor conditions.
- **Zeropole Neutrality:** A more static perspective, where zeros and poles coexist in a neutralized state, ensuring overall minimality and well-defined divisor properties.
- **Topological Zeropole Escape:** The hole-through-the-pole Absorption Principle maintains zeropole balance through a deep, higher genus topological transformation where certain finite singularities may be integrated into the core geometric structure across the compactified surface.

This framework serves as the guiding principle for the proof strategy, offering a consistent interpretation of various classical and modern approaches to analyzing the zeta function. Below, we enumerate the key instances where the Zeropole Balance Framework manifests within the proof, showcasing its versatility in uniting algebraic, geometric, analytic and topological perspectives.

- In Theorem 1, the Zeropole Duality and Neutrality principles manifest in the interplay between the Dirichlet pole at $s = 1$ in the $\zeta(1 - s)$ term and the zero introduced at $s = 0$ by the sine term $\sin\left(\frac{\pi s}{2}\right)$. This duality exemplifies the functional balance within the Riemann zeta function, where the placement of singularities across symmetric functional components ensures overall consistency under the functional equation.

- **Trivial Poles in the Hadamard Product (Theorem 2):** The modified Hadamard product explicitly introduces trivial poles at $s = -2k$ ($k \in \mathbb{N}^+$), balancing them with the trivial zeros arising from the functional equation. This balancing transformation ensures the analytic convergence of the infinite product while preserving the zeropole structure and preparing the next step in the proof.
- **Zeropole Duality of the Dirichlet Pole in (Theorem 2):** The $s(1-s)/\pi$ term in the Hadamard product encodes the dual role of the Dirichlet pole at $s = 1$, redistributing it into zero-like contributions at $s = 0$ and $s = 1$. This process preserves the functional symmetry inherent in the zeta function's structure and highlights the compensatory mechanisms that maintain balance within the framework.
- **Zeropole Mapping and Orthogonal Balance of $\zeta(s)$ (Theorem 5):** A fundamental component of the Zeropole Balance Framework is the dynamic and global pairing of zeros and poles, introduced through a bijective correspondence between the countably infinite trivial poles and non-trivial zeros. The perpendicular placement of trivial poles along the real axis and non-trivial zeros on the critical line encapsulates the geometric and algebraic interplay crucial to maintaining balance and enforcing minimality.
- **Zeropole Mapping and Orthogonal Balance of $\zeta^*(s)$ (Theorem 7):** The shadow function $\zeta^*(s)$ extends the zeropole balance framework by preserving the critical geometric and algebraic relationships of $\zeta(s)$ while ensuring toroidal compactification.
- **Dirichlet Pole Transformation in Shadow Function (Definition 1):** The Hadamard product's $\frac{s(1-s)}{\pi}$ term encodes the functional symmetry of s and $1-s$, ensuring the Dirichlet pole at $s = 1$ is mapped to a simple pole at $s = 0$. This preserves the zeropole balance framework while simplifying the divisor-theoretic analysis of $\zeta^*(s)$.
- **Hole-Through-the-Pole Absorption Principle:** The term $\frac{1}{s}$ introduces a simple pole at $s = 0$, which is absorbed into the torus hole, becoming an intrinsic part of the surface's geometry and contributing to the genus-dependent divisor computation. This absorption mechanism provides the clearest mathematical representation of the original orthogonal Zeropole Balance as a finite periodic divisor structure, that plays a fundamental role in this proof attempt.
- **Finite Degree of the Divisor (Section 6.5):** The finite nature of the divisor ensures that, within each periodic fundamental domain, the net degree computes to zero. This finiteness is crucial for the compactification approach, as it maintains a balanced and well-defined divisor structure across the entire surface.
- **Toroidal Embedding of the Shadow Function (Subsection 6.1):** The zeropole balance framework is compactified on a genus-1 toroidal surface, where periodic boundary conditions impose a structured repetition of the divisor pattern across the toroidal geometry. This construction maintains the fundamental balance of zeros and poles within each fundamental domain, demonstrating the adaptability of the framework to higher-genus compactifications while preserving minimality and avoiding accumulation issues.

- **Minimality and Exclusion of Off-Critical Zeros (Section 7.1):** The structured and finite fundamental domain divisor zeropole balance with a net-zero degree contribution ensuring that $\ell(D) = 0$ scales up to global zeropole cancellation, leading directly to the exclusion of off-critical zeros and reinforcing the necessity of the critical line.
- **Uniqueness of $\zeta^*(s)$ (Lemma 4):** The periodic constraints of the toroidal embedding impose a unique finite divisor structure, ensuring that $\zeta^*(s)$ is the only meromorphic function satisfying the required zeropole balance conditions.
- **Zeropole Directionality Invariance:** The framework accommodates both many-to-one and one-to-many mappings between zeros and poles while maintaining the same zeropole balance principle, as demonstrated by the theoretical fundamental domain structure allowing many-poles-to-one-zero mappings and practical numerical regions exhibiting many-zeros-to-one-pole patterns at higher heights.

These instances illustrate how the Zeropole Balance Framework permeates every stage of the proof, serving as the underlying mechanism that unites the algebraic, geometric, analytic, and topological components into a coherent and self-reinforcing structure. The framework does not merely provide a convenient interpretation but constitutes the essential guiding principle that enables the proof of the Riemann Hypothesis within the toroidal compactification approach.

13 Balanced Zeropole Collapse via Sphere Eversion

The finite periodic divisor structure of the zeropole framework reveals deep connections to sphere eversion—a topological transformation formalized by Smale in 1957 [Sma57] and visualized by Morin [Mor78]. This connection suggests a rigorous mathematical framework for studying singularity distributions through geometric transformations.

The periodic nature of our divisor structure provides natural "checkpoints" analogous to the key stages in Morin's sphere eversion process. Each fundamental domain maintains local zeropole balance while the global structure undergoes transformation, similar to how sphere eversion preserves smoothness despite complex local deformations.

This parallel suggests the following conjecture:

Conjecture 1 (Geometric Zeropole Invariants). *For any meromorphic function $f(s)$ with countably infinite zeros and poles admitting a toroidal compactification, there exists a finite set of geometric invariants $\{I_k\}_{k=1}^n$ preserved under continuous deformation of the fundamental domain, such that:*

1. Each I_k measures a specific aspect of zeropole balance across the fundamental domain.

2. The invariants remain constant during any smooth transformation preserving the periodic divisor structure.

3. The complete set $\{I_k\}$ uniquely characterizes the topological class of the zeropole distribution.

Furthermore, for the shadow function $\zeta^*(s)$, these invariants encode the minimal nature of its zeropole structure on the critical line.

This conjecture provides a framework for extending the zeropole analysis beyond the Riemann zeta function to a broader class of meromorphic functions. The geometric invariants would offer new tools for studying singularity distributions through the lens of differential topology, potentially yielding insights into other open problems in complex analysis.

The relationship between periodic divisors and Morin's stage-wise eversion process suggests these invariants might be computable through a finite sequence of local geometric measurements, similar to how sphere eversion is understood through its key intermediate configurations. This geometric approach to studying meromorphic functions could open new avenues for understanding the global behavior of complex functions through local topological properties.

This framework transforms the initial zeropole balance concept from a tool specific to the Riemann Hypothesis into a general mathematical approach for analyzing complex functions through geometric invariants. The existence of such invariants would provide a rigorous foundation for studying how singularity distributions behave under topological transformations while maintaining essential structural properties.

During the eversion process, distinct regions of the zeropole lattice progressively realign and collapse, reinforcing the algebraic neutrality of the toroidal structure. Crucially, this perspective reveals that while other meromorphic functions may admit toroidal compactification with countably infinite zeros, they would occupy fundamentally different spaces from $\zeta^*(s)$ due to its unique orthogonal zeropole structure. The special minimal nature of $\zeta^*(s)$ would be distinguished by specific values of these geometric invariants that no other configuration could achieve, thereby reinforcing rather than challenging its uniqueness in the proof of RH.

From this perspective, sphere eversion serves as a conceptual tool for understanding how the infinite zeropole balance extends into different topological and algebraic settings while preserving global minimality. The compactified framework of $\zeta^*(s)$ on the torus provides a natural setting for such transformations, reinforcing the fundamental algebraic and analytic structures underpinning the proof. This interpretation highlights the unifying nature of the zeropole framework, integrating geometric alignment, analytic continuation, algebraic independence, and topological flexibility in a way that places the Riemann zeta function's structure in a broader mathematical context while preserving its special character.

14 Historical Remark

The zeropole balance approach, as presented in this work, was not readily accessible in earlier formulations of the Riemann Hypothesis due to the historical evolution of the problem's analytical treatment.

In Riemann's original 1859 memoir [Rie59], the hypothesis was formulated in terms of the entire function $\xi(s)$, which excludes trivial zeros, trivial poles, and even the Dirichlet pole at $s = 1$. This choice was motivated by Riemann's primary focus on the critical line zeros, which play a fundamental role in prime number distribution. Consequently, the original number-theoretic objectives of Riemann's work led to an emphasis on the critical strip, inadvertently hindering the exploration of the broader complex-analytic structure of the zeta function.

As a result, the global interplay between trivial zeros and non-trivial zeros remained underappreciated, and the classification of trivial zeros as "trivial" further contributed to their overlooked significance in the global analytical structure. This historical perspective illustrates how a number-theoretic emphasis shaped the trajectory of Riemann Hypothesis research, delaying the recognition of a potential deeper geometric and algebraic balance within the function.

A notable example of zeropole balance can be observed in the formulation of $\xi(s)$, where the explicit presence of the gamma function term $\Gamma\left(\frac{s}{2}\right)$ effectively introduces trivial poles that neutralize the trivial zeros of the functional equation. In the formulation of the entire function $\xi(s)$, defined as:

$$\xi(s) = \frac{1}{2}s(s-1)\pi^{-s/2}\Gamma\left(\frac{s}{2}\right)\zeta(s),$$

the trivial zeros at $s = -2, -4, \dots$ are effectively neutralized by the poles of the gamma function term $\Gamma\left(\frac{s}{2}\right)$, ensuring that they do not contribute to the zero set of $\xi(s)$. As noted in Titchmarsh [THB86], this cancellation mechanism effectively removes the trivial zeros, reinforcing the notion that their role is one of algebraic and analytic balance rather than direct contribution to the distribution of prime numbers.

This historical insight highlights how the zeropole balance perspective provides a fresh interpretation of the classical formulation, revealing underlying structural symmetries that were historically obscured by the number-theoretic approach.

15 Acknowledgements

The author, an amateur mathematician with a Ph.D. in translational geroscience, extends heartfelt gratitude to OpenAI's ChatGPT-4 for providing critical insights, mathematical

knowledge, and assistance in proof formulation, significantly expediting the process. Special thanks to Professor János Kollár, algebraic geometer, for flagging an issue in the original proof leading to the construction of the shadow function and Adam Antonik, Ph.D., for his probing questions that helped refine the proof. The author extends gratitude to Boldizsár Kalmár, Ph.D. on how to present the manuscript for the professional mathematical community. Any errors or inaccuracies in the proof attempt remain the sole responsibility of the author.

16 Supplementary Material

The code for the numerical evaluation of the exponential stabilizer of the shadow function and related plot generation is provided in the Jupyter Notebook `Supp_Mat_Stabiliser_Eval.ipynb`. Additionally, the code for generating the Numerical Validation of Dynamic Zero-Pole Pairing is available in the Jupyter Notebook called `Supp_Mat_Num_Val_Dynamic_ZeroPole_Pairing.ipynb`. Both files are available at GitHub at https://github.com/attila-ac/Proof_RH_via_Zeropole_Balance.

17 License

This manuscript is licensed under the Creative Commons Attribution-NonCommercial 4.0 International (CC-BY-NC 4.0) License. This license allows others to share, adapt, and build upon this work non-commercially, provided proper attribution is given to the author. For more details, visit <https://creativecommons.org/licenses/by-nc/4.0/>.

References

- [Eul37] Leonhard Euler, *Variae observationes circa series infinitas*, *Commentarii academiae scientiarum Petropolitanae* **9** (1737), 160–188.
- [Gow23] Timothy Gowers, *What makes mathematicians believe unproved mathematical statements?*, *Annals of Mathematics and Philosophy* **1** (2023), no. 1, 10–25.
- [Had93] J. Hadamard, *Etude sur les propriétés des fonctions entières et en particulier d’une fonction*, *Journal de Mathématiques Pures et Appliquées* **9** (1893), 171–216.
- [Har14] G.H. Hardy, *Sur les zéros de la fonction zeta de riemann*, *Comptes Rendus de l’académie des Sciences* **158** (1914), 1012–1014.
- [Mir95] Rick Miranda, *Algebraic curves and riemann surfaces*, Graduate Studies in Mathematics, vol. 5, American Mathematical Society, Providence, RI, 1995.

- 1093 [Mor78] Bernard Morin, *Sphere eversion*, Presses Universitaires de France, 1978.
- 1094 [Mun00] James R. Munkres, *Topology*, Prentice Hall, 2000.
- 1095 [Rie59] B. Riemann, *Über die anzahl der primzahlen unter einer gegebenen grösse*, Monats-
1096 berichte der Berliner Akademie, (1859), 671–680.
- 1097 [Sma57] Stephen Smale, *A classification of immersions of the two-sphere*, Transactions of
1098 the American Mathematical Society **90** (1957), no. 2, 281–290.
- 1099 [Tao08] Terence Tao, *Compactness and compactification*, The Princeton Companion to
1100 Mathematics (Timothy Gowers, June Barrow-Green, and Imre Leader, eds.),
1101 Princeton University Press, Princeton, 2008, pp. 167–169.
- 1102 [THB86] E. C. Titchmarsh and D. R. Heath-Brown, *The theory of the riemann zeta-function*,
1103 2nd ed., Clarendon Press, Oxford, 1986, With a preface by D. R. Heath-Brown.